Bolm Inst. oceanogr., S Paulo, 31(1):11-32, 1982

SEASONAL CHARACTERISTICS OF HYDROGRAPHY, TURBULENCE AND DISPERSION NEAR ILHA GRANDE (RJ), BRAZIL, BASED ON R/V "PROF. W. BESNARD" DATA

Yoshimine IKEDA[1] & Merritt Raymond STEVENSON[2]

1 Instituto Oceanográfico da Universidade de São Paulo

2 Instituto de Pesquisas Espaciais, CNPq

Synopsis

Seasonal differences in sigma-t (1.8), temperature (4.0°C) and salinity (0.9°/oo) were observed during February/June 1976 in the vicinity of Ilha Grande off the coast of Brazil. Estimates of static and dynamic stability were made through the calculation of Brunt-Väisälä frequencies and Richardson numbers, respectively. Both static and dynamic stability values were larger in February than in June for the same location and suggest a greater column stability in February than in June. Stations located in the northern and western channels of Ilha Grande, however, contained greater density reversals than to the east of the Island. Small scale dispersion studies were made using Rhomamine B dye to determine horizontal diffusion coefficients (K) east of the Island and in an embayment of the Island. The estimate for K was $9X10^3$ cm^2 s^{-1} east of the Island, about 2.6 times greater than the value estimated for the protected embayment.

Introduction

Ilha grande lies across the entrance to Ilha Grande Bay and its presence there can be expected to affect the circulation and mixing processes in the bay. It is the interaction of time variant currents such as tidal currents with the general nearshore currents that give rise to the biological productivity found both in the bay and near the Island. Tommasi *et. al.* (1972), Miranda & Ikeda (1976), Miranda *et al.* (1977), Signorini (1980*a,b*), Ikeda & Stevenson (1980), have discussed biological and environmental aspects of the oceanography of the area. Another report by Ikeda & Stevenson (1978) discusses temporal and spatial variability in sea surface temperature for the region encompassing Ilha Grande as measured from a NOAA satellite. That study, however, was not so spatially detailed as this report. This paper will discuss the distribution and variability of currents measured at various locations in the bay over short time periods, in conjunction with hydrographic data dye dispersion measurements, during two seasons, to obtain a better understanding of the dynamic processes operating in the bay and near Ilha Grande.

Work at fixed oceanographic station number 1 was carried out at 1-hour intervals in February 1976. In June 1976, for the stations numbers 2, 3 and 4, the sampling frequencies were at 2-hour intervals. Temperature, salinity and current measurements were made from the surface to the proximity of the bottom at each station. The fixed stations are plotted in Figure 1. All references to time are in GMT.

Analysis of hydrographic and current meter data

Great variation was observed in temperature, salinity and sigma-t (Fig. 2) at fixed oceanographic station number 1 in February. A surface mixed layer of temperature extended from 0 to 15 m depth while halocline and pycnocline were apparent only from 15 m to the bottom, from 17:00 to the end of the observations. The biggest sigma-t (24.0) corresponding to a temperature and a salinity of 20°C and 35°/oo respectively, occurred close to the bottom, from 17:00 to the end of observations. The smallest sigma-t (22.2) was associated with a temperature of 26.3°C and a salinity of 34.0°/oo and occurred at the surface layer.

The analysis of current diagrams (Fig. 3) for February shows inflow from 05:00 - 08:00 and outflow from 08:00-17:00. Inflow occurred again from 17:00 to 19:00 and outflow from 20:00 until the end of observations. Current

Publ. nº 528 do Inst. oceanogr. da Usp.

strength was generally greatest at 8 ~ 14 m depth.

From temperature, salinity and sigma-t (Fig. 4) time series for the June Cruise at the same location (station 2) a decrease of temperature occurred from 12 m depth to the bottom between 02:00 and 08:00, along with an increase of salinity in this interval of time. The contribution from temperature and salinity changes in turn gave rise to increases in sigma-t during this period. This decrease in temperature is associated with an increase in salinity over the same depth and suggests a thermal structure change caused by advective processes. Consequently the increase of density with depth at the same time interval reflects changes in thermal and saline structures. From 08:00 till the end of the observations, there was little change in the thermal and saline water inflow.

Analysing current diagrams, shown in Figure 5 for fixed station 2, we see inflow from 02:00 (beginning of observations) to 05:00. Outflow occurred from 05:00 to 12:00, inflow from 12:00 to 18:00 and outflow until the end of observations. Strong currents were observed at 4 ~ 12 m depth.

The largest sigma-t (24.0) (Fig. 4), was observed between 02:00 - 08:00 and 16:00 - 18:00 (T = 22.2°C and S = 34.7°/oo) during inflow. The smallest sigma-t (23.7) (T = 22.7°C and S = 34.5°/oo) was observed between 00:00 and 03:00.

From data analysis for the upper layer of stations 1 and 2, for the February 1976 Cruise we can say that the temperature remained about 26.3°C, the salinity 34.0°/oo and sigma-t 22.2. For the June 1976 Cruise, the variation in sigma-t was from 23.7 to 24.0, temperature went from 22.1°C to 22.7°C and the salinity from 34.5°/oo to 34.9°/oo.

At 17:00 during February (Figs 2 - 3), there is an entry of cool and relatively high salinity (34.8 ~ 35.0°/oo) oceanic water into the area. This inflow occurs from 12 to 20 m depth and corresponds in the velocity field to a maximum current of 42 cm s^{-1} (V_x, V_y = 30 cm s^{-1}) at 12 m, the strongest flow observed during the time series. A weak surface front containing cooler and more saline water extending the stable area at about 01:00.

We can see from Figures 4 and 5 that again in June there is an intrusion of cooler and higher salinity water. This occurs first at ≥ 12 m depth for a several hour period and corresponds to a velocity reversal in both V_x and V_y components. That is, during this period of 01:00 - 09:00, there is a basic shift in the direction of flow. From about 12:00 to the end of the observation period, we again see a significant change in the water column as an oceanic front passes through the area. This is evidenced as the slope of isotherms, isohalines and isopycnals become vertical and represent a "wall" or frontal interface. The water that was about 22°C and

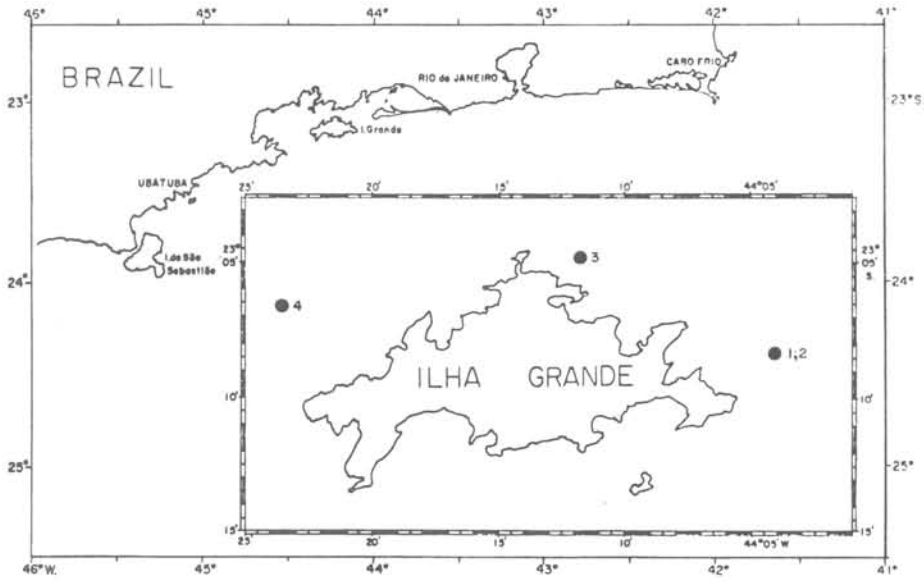

Fig. 1. Fixed station positions.

at ≥ 12 m depth is now essentially near the surface and the temperatures are vertically isothermal. Also corresponding to this time of frontal passage, we see a subsurface jet-like flow (40 cm s^{-1}) centered at 8 m depth associate with the frontal passing, followed by reduced velocity and a change in direction of flow.

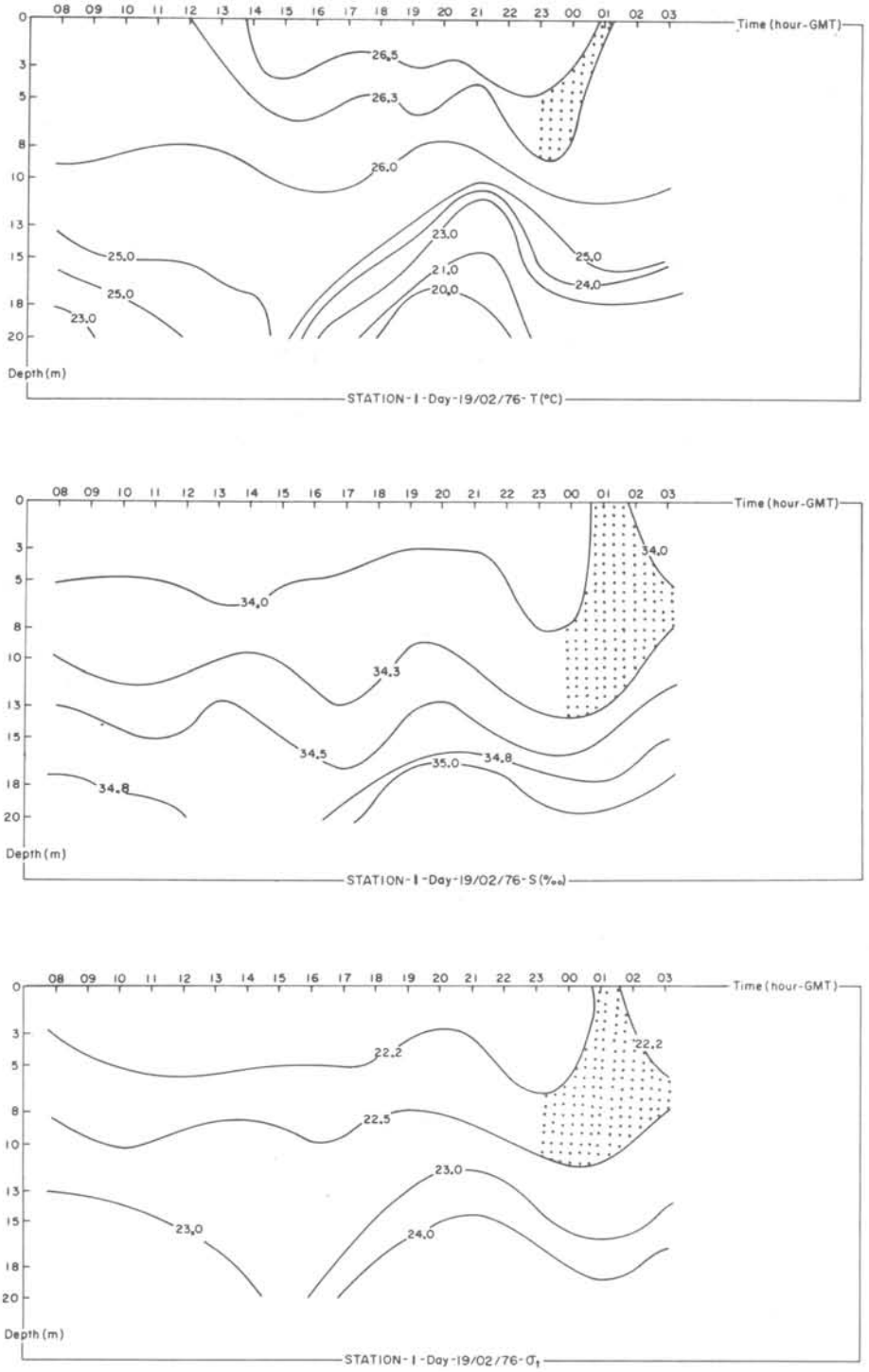

Fig. 2. Temperature, salinity and sigma-t time series (Fixed Station 1).

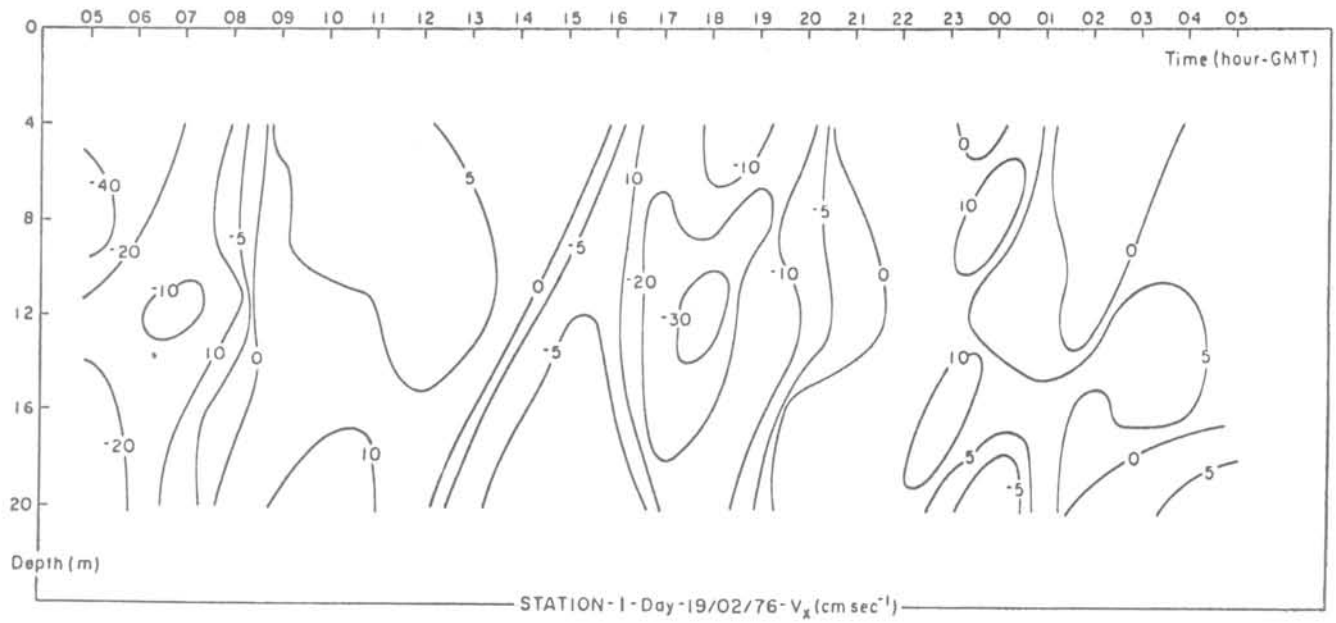

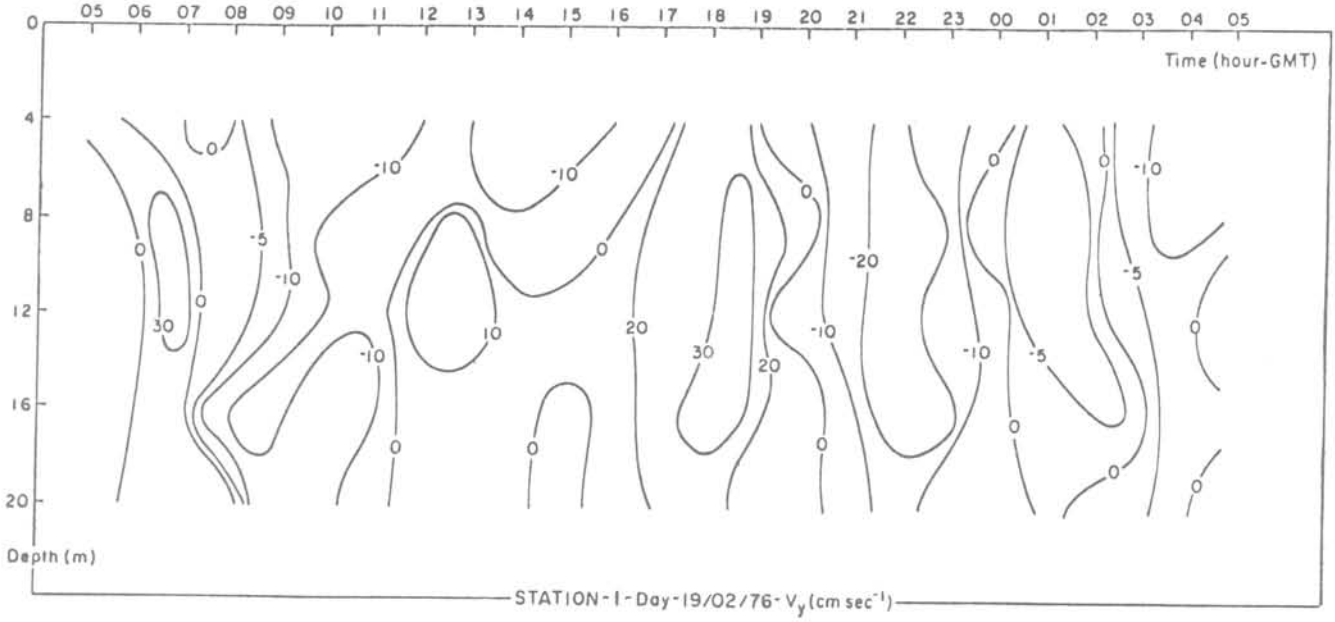

Fig. 3. Current time series (fixed station 1): V_x and V_y components, positive to east and north, respectively.

A comparison of stations 1 and 2 for the two different seasons suggests that subsurface oceanic water often may enter into the area. During both seasons a subsurface flow preceeded a surface frontal passage. In June, we observed a frontal passage that extended from the surface to at least 20 m depth. A weak front appears to have been present in the February data but extending from the surface to only 10 m depth. The water flow at the front was also correspondingly weaker than during the June observation period.

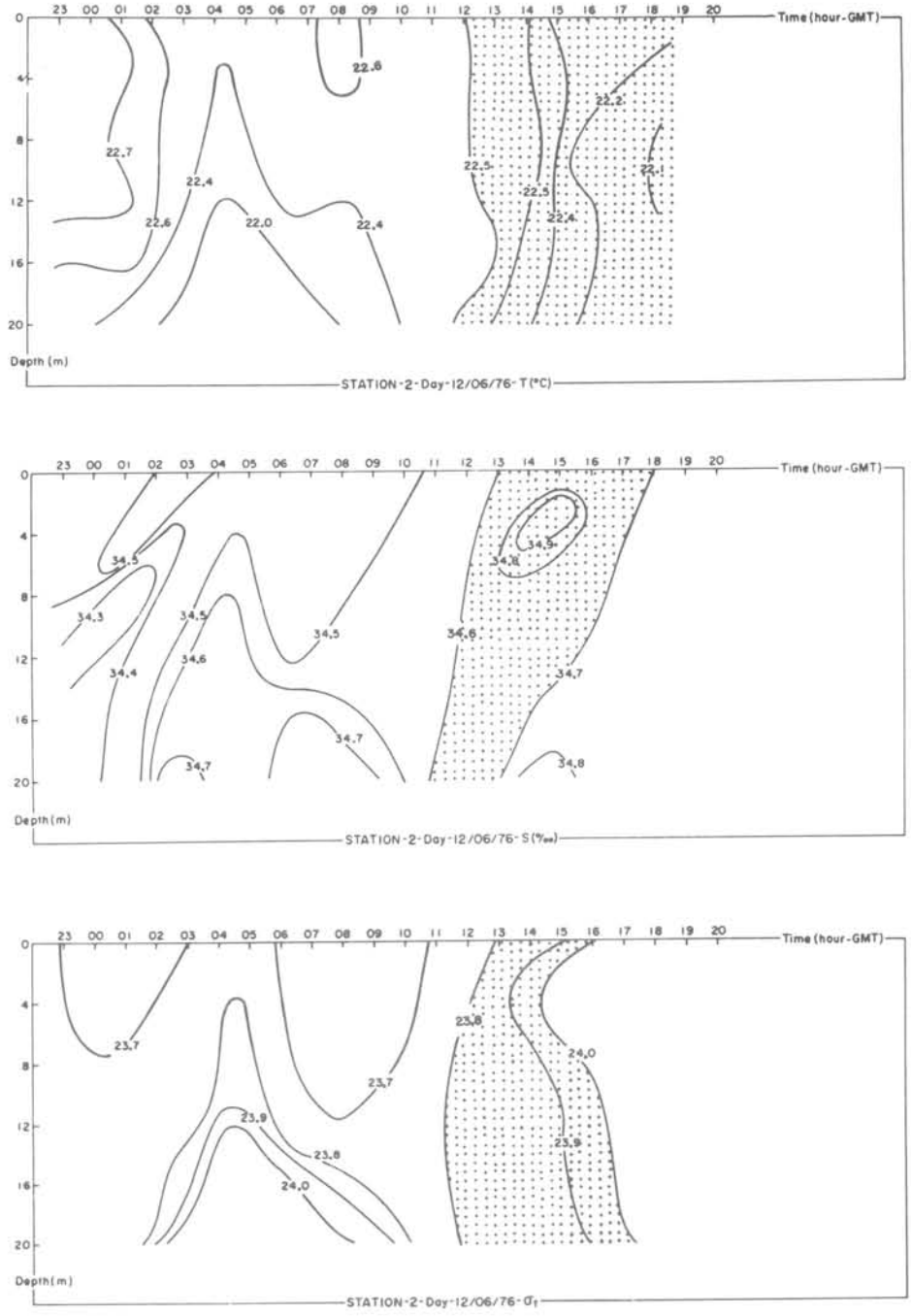

Fig. 4. Temperature, salinity and sigma-t time series (Fixed Station 2).

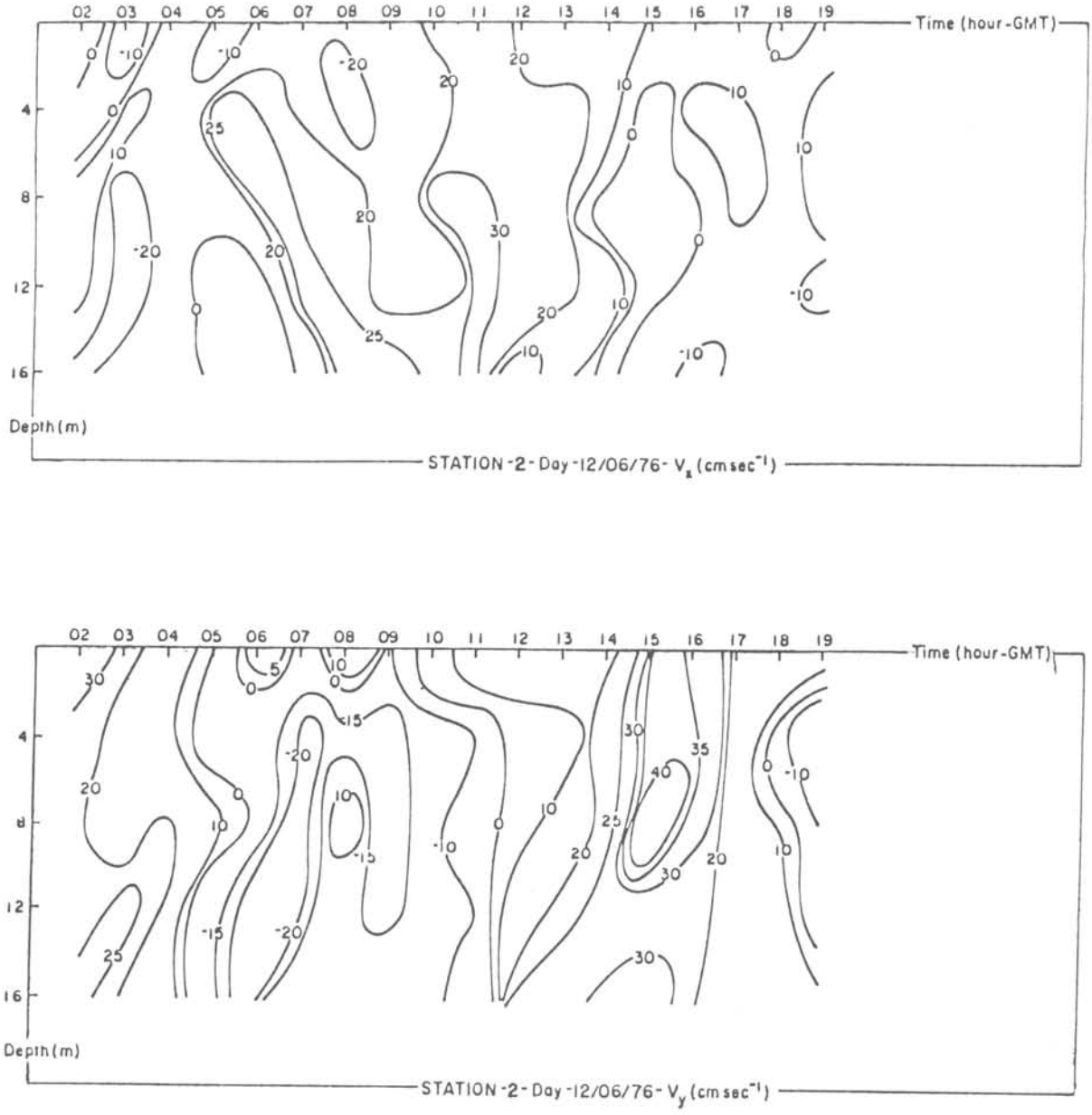

Fig. 5 Current time series (fixed station 2): V_X and V_Y components positive to east and north, respectively.

It is observed from the temperature, salinity and sigma-t time series of fixed station number 3 (Fig. 6), located in a channel on the northern side of Ilha Grande, that the largest variations in sigma-t occurred at 03:00 and 08:00. For this period, temperature variations occurred from the surface to the bottom and salinity varied but little.

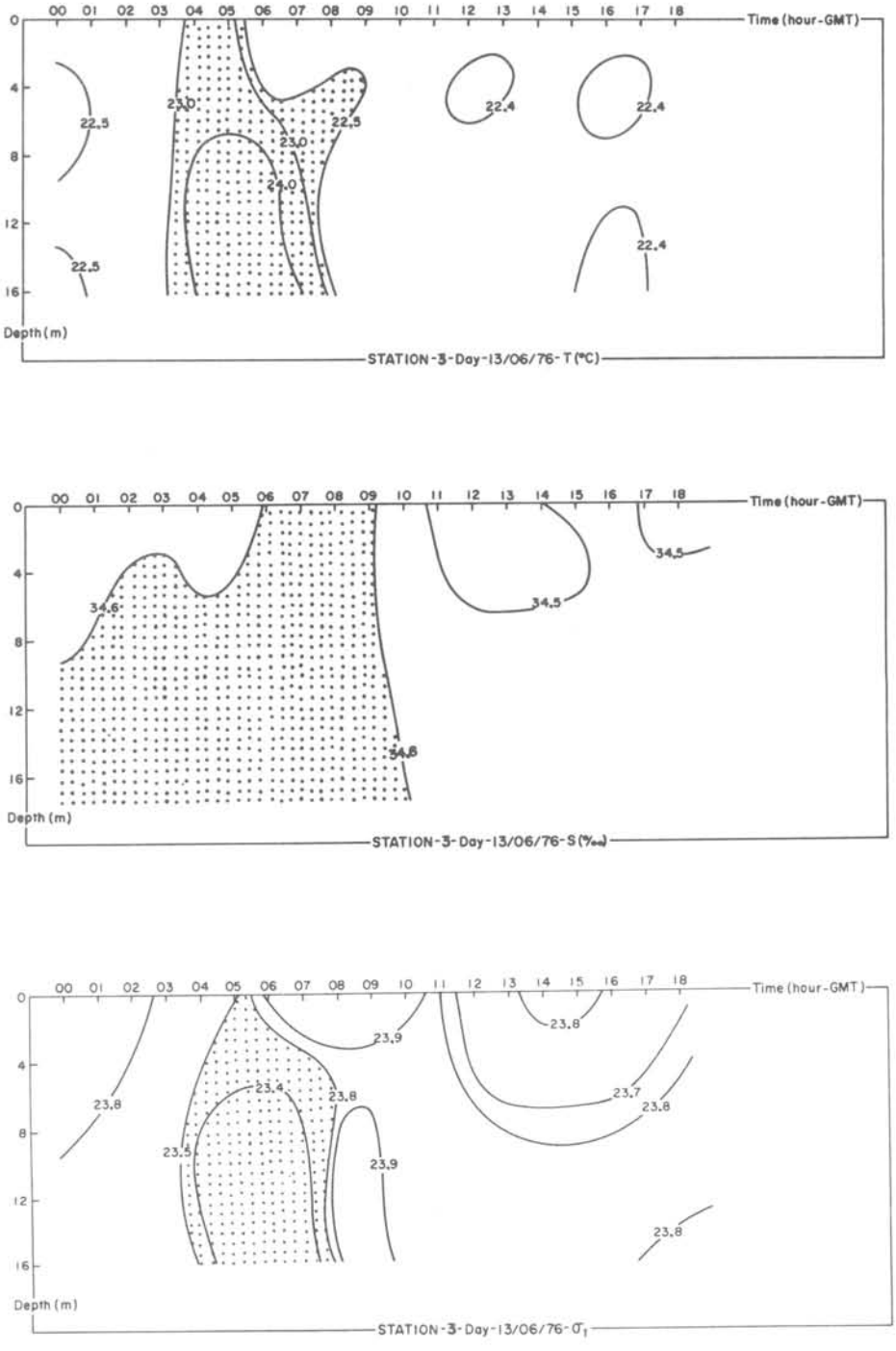

Fig. 6. Temperature, salinity and sigma-t time series (Fixed Station 3).

Analysing current diagrams (Fig. 7), it is seen that during the observation period, the current maintained one direction and that the velocity was more intense between 03:00 and 08:00 than other times. Variation of velocity with depth occurred principally in the V_y component where the strongest velocities were at 8 ~ 16 m depth. The largest sigma-t (23.9) was observed between 06:00 and 11:00 (T = 22.5°C and S = 34.6°/oo). The smallest sigma-t (23.4; T = 23.0°C and S = 34.6°/oo) occurred between 04:00 and 07:00.

From the vertical time series of station 3, we also see the passage of a front. In this instance the frontal structure is more complex. From the thermal field we see a "thermal wall" pass between 03:00 to 09:00 where the wall extends from the surface to 16 m depth. The salinity feature is not so well defined, although from 06:00 to 09:00 the water column is largely isohaline from the surface to 16 m. The sigma-t field shows the frontal passage to occur at about 03:00 and to continue until about 08:00. What makes this frontal feature different from station 2 is that the frontal water was warmer and consequently of lower density than the water preceeding or following. While the greater salinity (34.6°/oo) partially offsets the effect of warmer water temperatures, the thermal characteristics are still dominant as seen in the sigma-t field. It is possible that this may not be a front but sort of a lense of warmer water that is passing through the area. The data show the passage to correspond with a velocity maximum for 04:00 ~ 06:00.

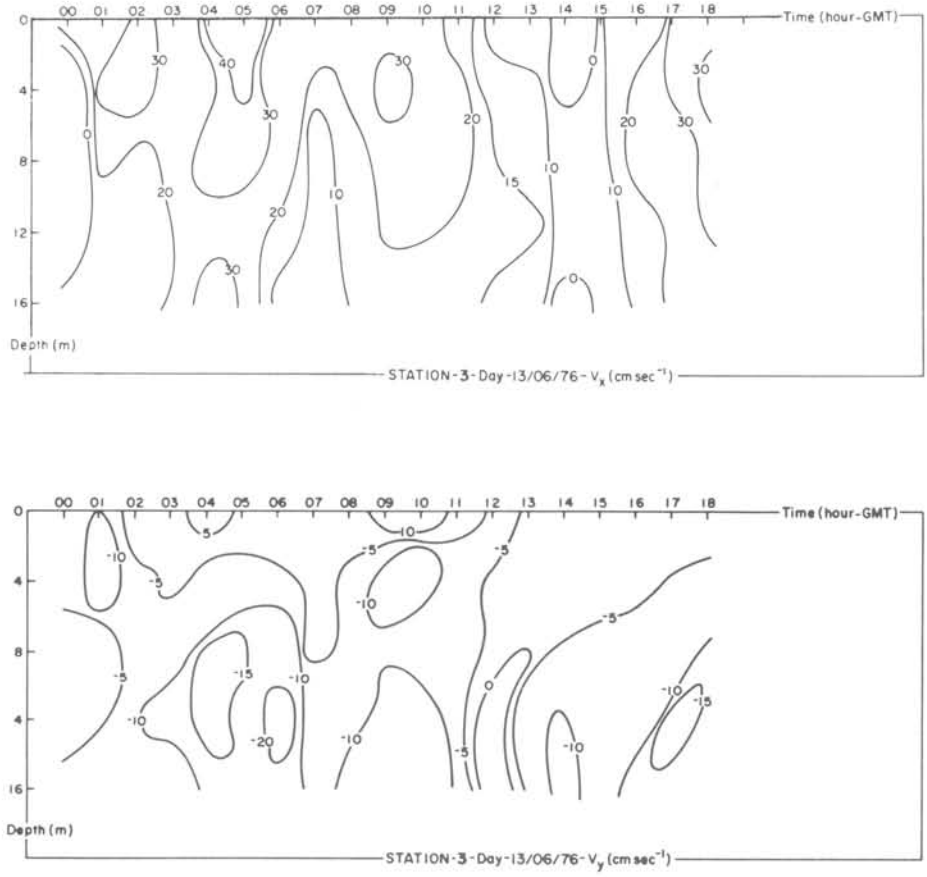

Fig. 7. Current time series (fixed station 3): V_x and V_y components positive to east and north, respectively.

At fixed station number 4 using temperature, salinity and sigma-t (Fig. 8) time series, only the temperature presented much variation.

The analysis of current diagrams (Fig. 9) shows a predominant inflow. A stronger current flow is found at depths between 6 m and 14 m.

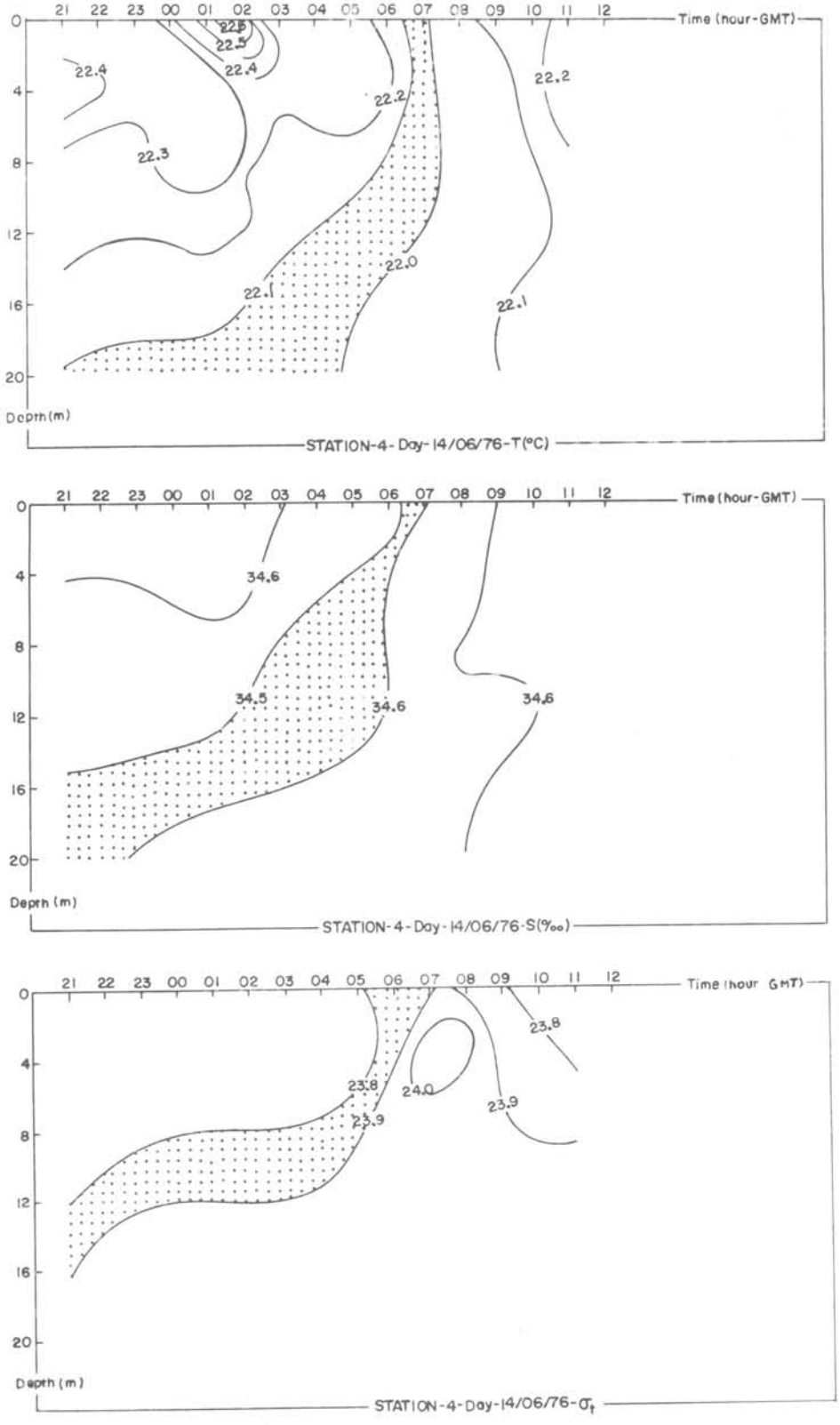

Fig. 8. Temperature, salinity and sigma-t time series (Fixed Station 4).

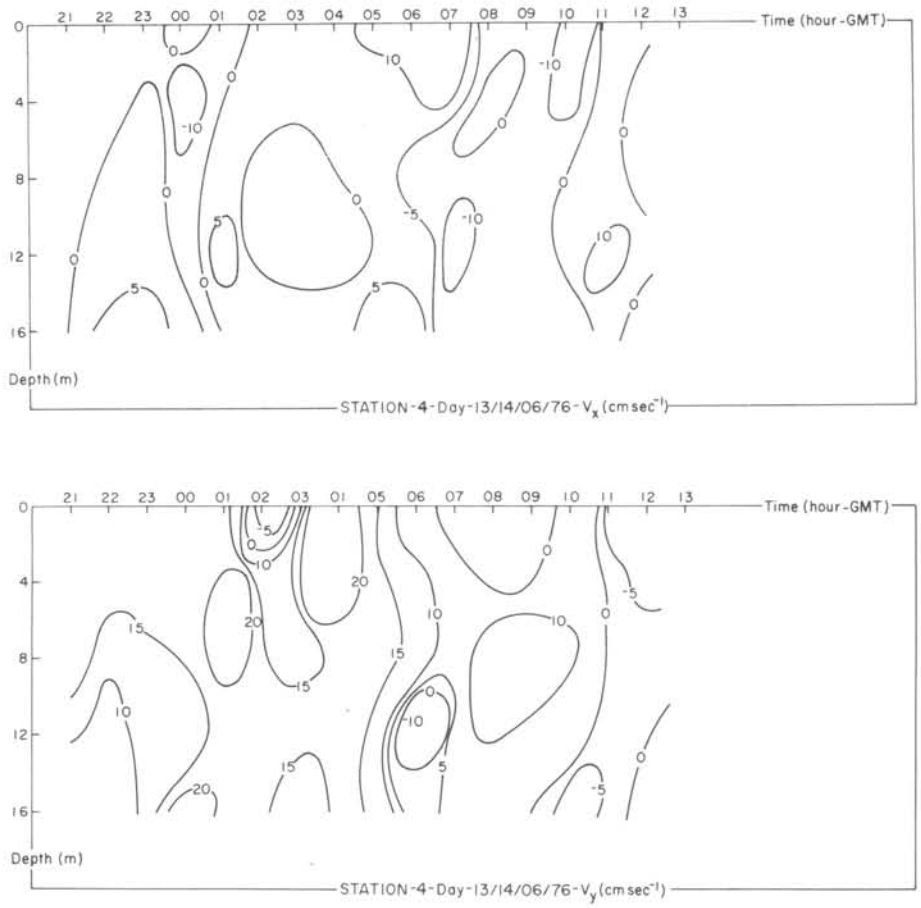

Fig. 9. Current time series (fixed station 4): V_x and V_y components positive to east and north, respectively.

Station 4 is at the western end of the channel separating Baía da Ilha Grande from Baía de Sepetiba and variation in the water properties are expected to indicate an exchange between the two bays. From the temperature time series (Fig. 8) we can see that a front begins to enter the area toward the end of the measurement period (06:00 onward). The salinity field, however, varies but slightly. The density field therefore is determined primarily from the temperature distribution and we can see what appears to be a frontal passing, followed by the entrance of a thin surface layer (0 ~ 6 m) of warmer, less saline water commencing about 08:00 and until the end of the measurement period.

A comparison of current speed data with T,S and sigma-t time series shows correspondence of change in velocity with passage of the surface frontal feature. Subsurface velocity features are found just beneath the pycnocline that separates the more coastal water from the more oceanic water.

Fronts or the passage of frontal interfaces, were apparent in all the 4 fixed stations. At the first station the surface front was warm (26.3~26.5°C) and of relatively low salinity (34.0~34.3°/oo). For station 2 the surface front was 22.0~22.5°C and 34.6~34.7°/oo; for station 3 the front was 22.5~24°C and about 34.6°/oo; and for station 4 the front was 22.0~22.1°C and largely isohaline at 34.5°/oo. The front observed in February (station 1) contained significant variation in both temperature and salinity, while those of the June season were primarily thermal features with little salinity change. The similarity between the sigma-t time series and temperature series supports this interpretation.

Comparison of current meter and tidal prediction data

To obtain a better understading of the characteristics of circulation in the study area, tidal height prediction calculations were made for the February and June 1976, observational periods (Fig. 10) and referenced to the nearby coastal city of Angra dos Reis (Brasil, 1975). The part of the tidal prediction curves that correspond to the 4 fixed stations are also seen in Figure 10.

A comparison of the Angra tidal curve with the current meter data for February (station 1; Fig. 3) suggests that the fluctuation of currents is much more complex than that suggested by the tidal fluctuation as has been noted by Ikeda & Stevenson (1980). The V_y component of the velocity field appears to fluctuate at about twice the frequency of the tidal oscillation and Ikeda & Stevenson note that oscillations of about 6 hours were present in the current meter records.

The situation for June (station 2 at the same location) shows the V_y flow to correspond well with the ebb and flow of the concurrent tidal cycle; station 2 current data appears to follow the tidal curve better than during the February observation period.

For station 3, the meridional magnitude of the current flow would be expected to be smaller than the zonal component (V_x) because the proximity of Ilha Grande effectively limits the meridional flow. The comparison of the tidal curve with the current meter series suggests that while the tidal height peaked shortly after the start of the observational period and continued to ebb for most of the period, the current flow was essentially in an eastward direction with no reversal in direction even while the tidal height began to increase again. This suggests that the observed (zonal) flow is a consequence of the pumping action of water from west to the east through the channel separating the two adjacent bays.

The current pattern suggests a "rectified" flow, that is, the current does not reverse in direction but diminishes and aproximates zero velocity before increasing again in the same direction.

Station 4 lies to the northwest of Ilha Grande and as a result reflects motion both in the direction of Angra dos Reis and in the channel separating the two bays. The flow remains fairly strong to the north before, during and after peaking of tidal height where upon the flow northward decreases during the next 8 hours while the tide ebbs and begins to build again. This pattern suggests that the increasing tidal water upon leaving the Angra area flows predominantly through the channel rather than out to sea past station 4.

One explanation for the short period pulsation observed in the current meter time series has to do with basin geometry. Another possible cause of the high frequency oscillations may have to do with the tidal progress into the channel from both sides of Ilha Grande.

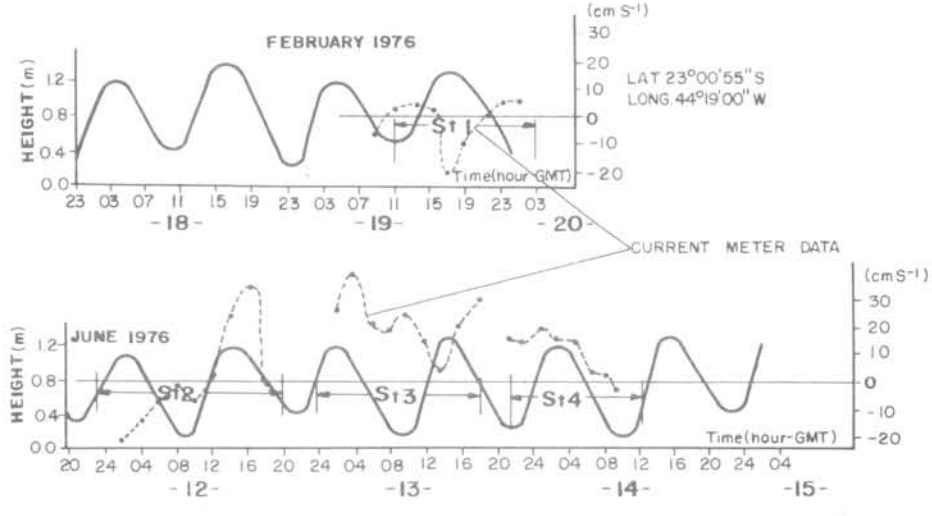

Fig. 10. Tide prediction for Angra dos Reis.

Due to differences in depth and path lenght, oscillations may propagate into the channel in opposing directions and slightly different periods and phases.

Static stability and Richardson number

When water movements involve great masses such as in an ocean, a bay or in large channels, where the fluid is not homogeneous, the density stratification effects of the fluid mass must be taken into account in the discussion of their movements and in their distribution of properties. Turbulence and hence dissipation of turbulent energy is promoted if the density stratification on horizontal turbulent movements is much smaller than the effects of inertia and horizontal pressure gradients.

Estimates were made of both static and dynamic stability. Static stability was computed for each of the 4 fixed stations using the Brunt-Väisälä frequency equation (1) (Phillips, 1966).

$$N = \left(\frac{g}{\rho}\frac{\partial \rho}{\partial z} - \frac{g^2}{c^2}\right)^{1/2} \qquad (1)$$

Where: g - acceleration of gravity
ρ - density of sea water
z - depth below sea surface
c - velocity of sound in water

In practice, a large value for N implies a highly stratified water layer which in turn indicates that a parcel of water vertically displaced from its initial position will tend to quickly return to its original position due to a buoyant restoration force. Small values of N however, indicate a tendency to return to the original position but much more slowly. Negative values in the argument of equation 1 indicate a turbulent overturning of the water in that part of the column so affected.

A look at station 1, static stability (Fig. 11) for February suggests that static stability was greatest (N = 5 cph) below 10 m beginning at 17:00 and continuing until the end of the observation period. This stratification was due to oceanic water entering the area at that time. Small values of N were about 3 cph, still reasonably stable for the water column.

Conditions were markedly different at the same location in june (Fig. 12). At that time we see a maximum value for N of about 3 cph and decreasing to 0. In some levels, the argument of the Väisälä equation was negative and is shown here as a shaded zone. In these zones, physical overturn of water in that part of the water column is promoted with release of large amounts of turbulent energy.

Similar conditions of static instability are indicated for station 3 (Fig. 13) where the largest Väisälä frequency is about 4 cph and decreases to 0. Again, depths of density reversal are present and indicated by the shaded areas.

For station 4 (Fig. 14) northwest of Ilha Grande, reduced and 0 values of N are encountered, together some unstable zones. The largest value of N is about 3 cph. Although station 4 contains unstable water conditions, the strongest instability occurred at station 3 for a 2-hour period at 4 m depth. The shaded zones may be considered to be locations where even if no horizontal currents were present, density instabilities present would produce pulses of turbulent energy in the form of vertical motion and mixing of water in the column.

The restoring buyoant force indicated from the magnitude of N can also be interpreted as related to passage of internal waves (Smith, 1978), since such vertical dislocation of a water parcel will result in the parcel oscillating vertically as it progressively returns to its original position. The fundamental mode of oscillation is given by the Väisälä frequency N. The vertical movement and horizontal propagation of this oscillation is essentially indistinguishable from that of internal waves of the same frequency passing by the point of observation.

Ikeda & Stevenson (1980) noted the frequent occurrence of short period oscillations in the current meter records (1 ~ 1.1 cph). Inspection of the 4 stations in this paper shows that for February (station 1), the Väisälä frequency was $\geq$ 3 cph. Energy propagating into the area in the frequency of an 1-hour periodicity would represent a forced motion since the water column would not naturally support such an oscillation. During June, however, stations 2, 3 and 4 contain Väisälä frequencies $\leq$ 3 cph so the water column would be expected to support (or resonant with) the periodicities observed in the current meter records.

Phillips (1966) also showed that vertical stability of a fluid in motion depends on the following non-dimensional parameter called Richardson number (Ri):

$$Ri = \frac{\frac{g}{\rho}\frac{\partial \rho}{\partial z}}{\left(\frac{\partial v}{\partial z}\right)^2} \qquad (2)$$

where: g - acceleration of gravity
ρ - density
v - velocity of water

In equation 2 the numerator is referred to as the static stability term, which divided by the vertical velocity shear provides and indication of the dynamic stability (or unstability). We can therefore relate the following criteria due to Miller & Howard (Phillips, 1966), for situations in which vertical instabilities (turbulence) occur.

If $Ri < 0.25$, the movement is vertically unstable and therefore fluid motion is converted into turbulent motion.

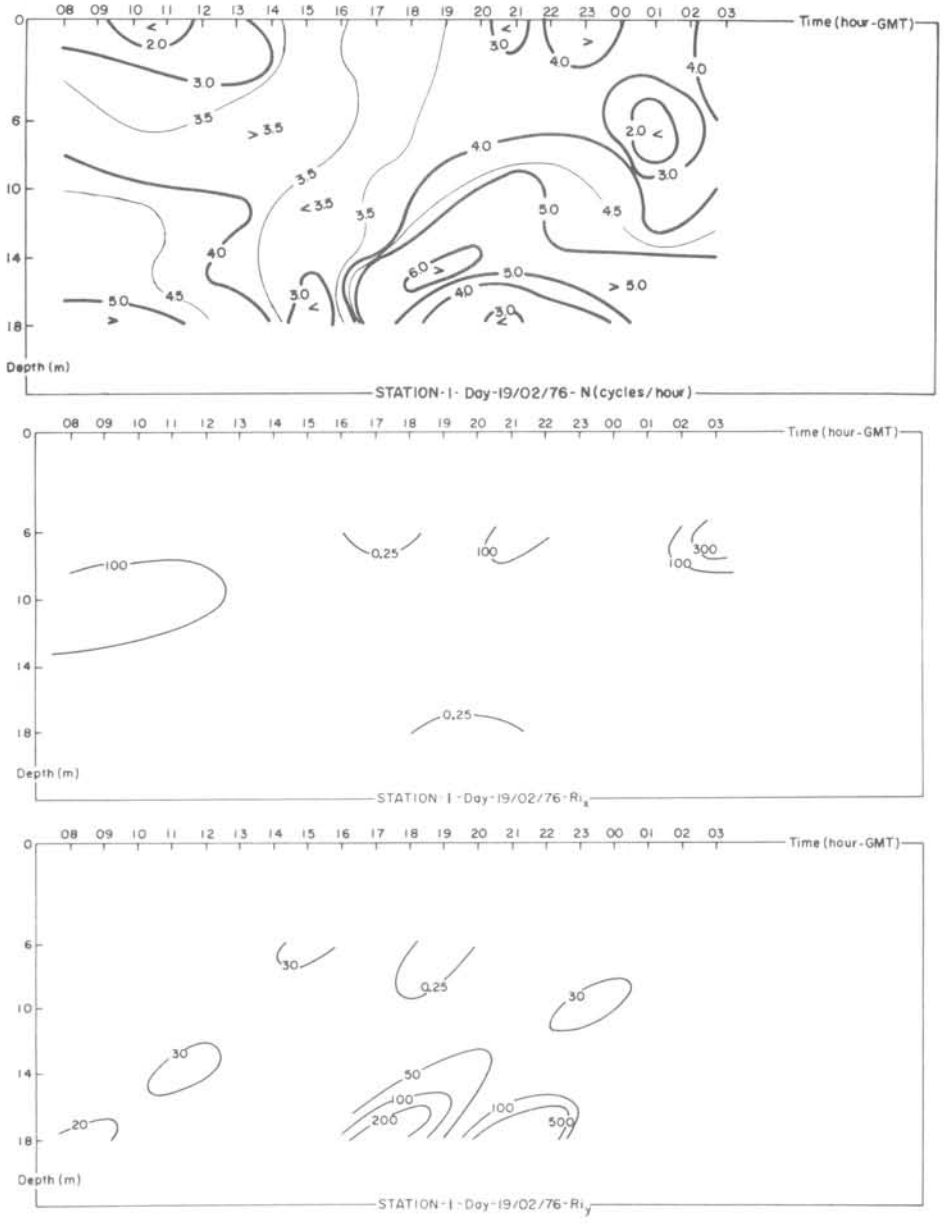

Fig. 11. Brunt-Väisälä frequency and Richardson number time series (Fixed Station 1).

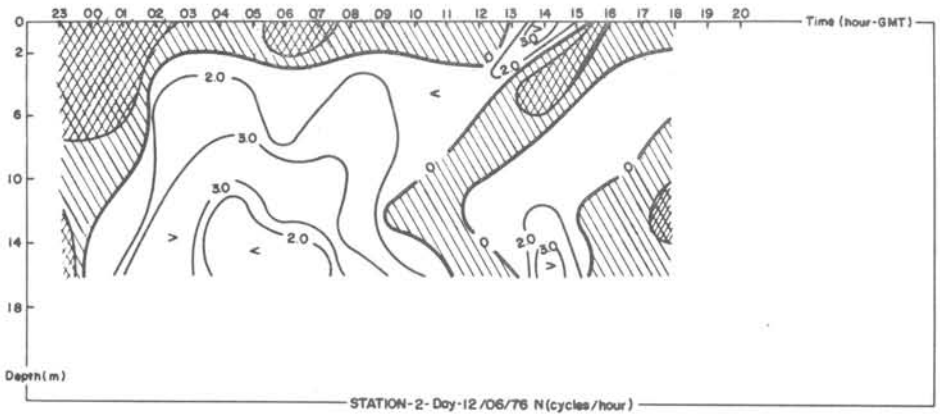

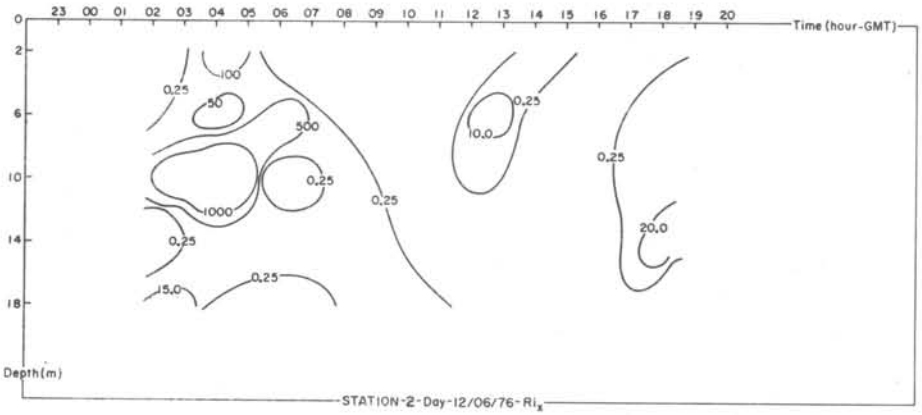

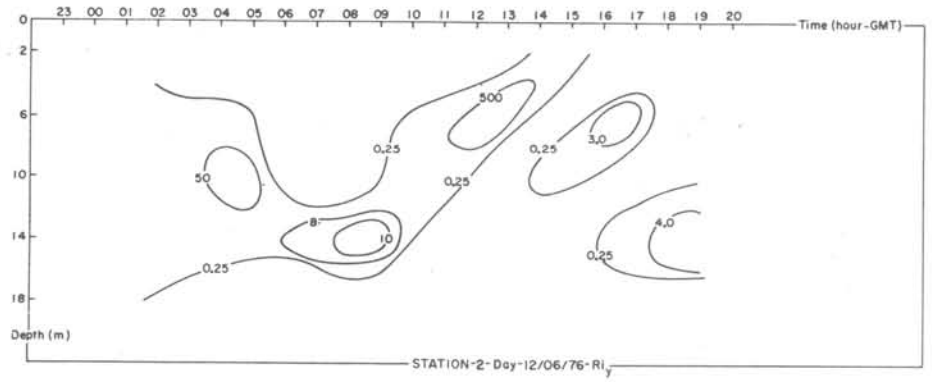

Fig. 12. Brunt.Väisälä frequency and Richardson number time series (Fixed Station 2).

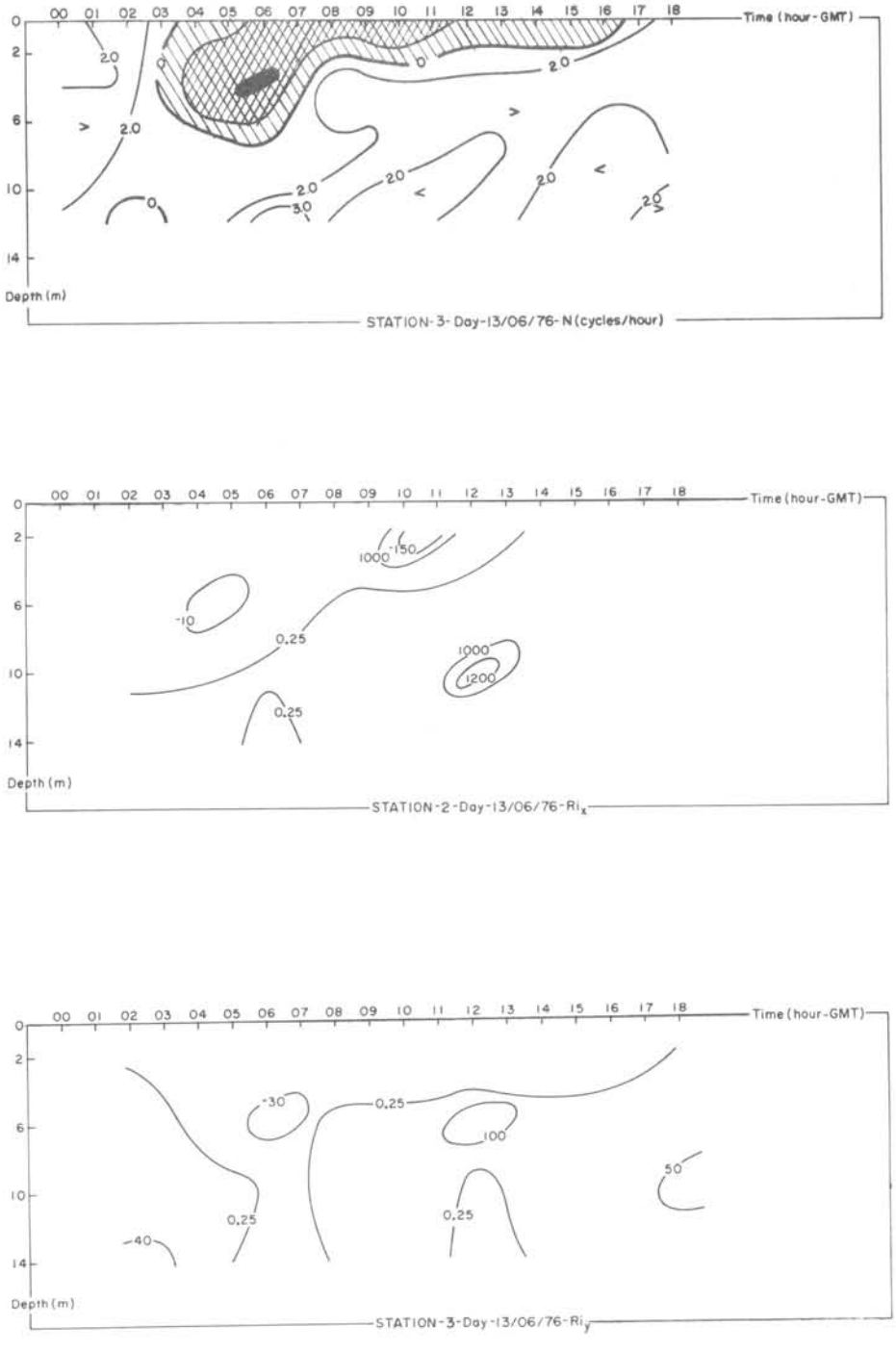

Fig. 13. Brunt-Väisälä frequency and Richardson number time series (Fixed Station 3).

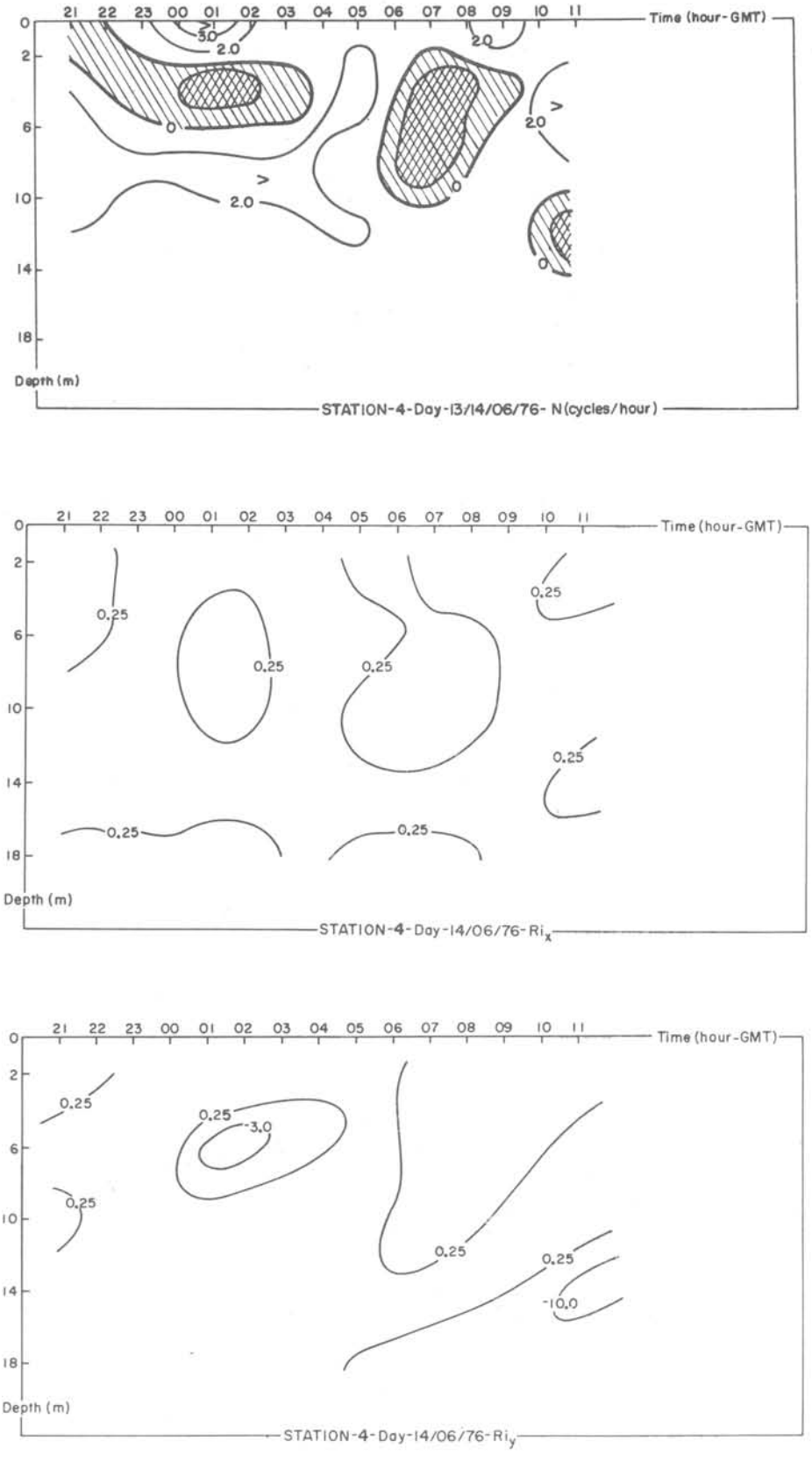

Fig. 14. Brunt-Väisälä frequency and Richardson number time series (Fixed Station 4).

From sigma-t data and the current meter observations we determined Richardson number time series for different depths for the fixed stations. In Figures 11 - 14 we show spatial and temporal variation of the Ri parameter (in Ri_x and Ri_y component form) for the 4 stations. From Figure 11 we see that the more turbulent region occurred between 15:00 and 21:00 through the water column for the Ri_x (zonal component) and in the upper 10 m layer for the north/south component. The turbulent regime occurred during the same period as when the maximum velocities occurred (Fig. 3). The Ri_y values show the greatest instability just beneath the surface layer, corresponding to a thermal range of 26.0 ~ 26.3°C and just above the 34.3°/oo isohaline. Frequently fronts may contain zones of strong current shear which, when combined with weak static stability, produce dynamic instability. This is not unexpected since the frontal interfaces are regions of maximum momentum exchange and mixing. A strong velocity gradient must be present if the observed gradients are to be maintained. Passage of the surface front at 01:00 however, didn't correspond to low Ri values, because there was apparently little current meter shear.

For station number 2 (Fig. 12), it is possible to observe dynamic instability in the upper layer which reaches greater depth between 05:00 and 10:00 in the outflow. Instability or enhanced conditions for turbulent dissipation are also found in a bottom layer which is not greater than 5 m, except from between 09:00 and 15:00 when the layer thickness increases up to within 4 m of the surface. The low Ri_y numbers that extend in a band from about 06:00 to 16:00 correspond well with the 35.5 ~ 35.7°/oo isohalines which generally represent stronger salinity gradients. The small Ri_x component values tend to correspond with thermal gradients or frontal features.

The Ri distributions for station 3 (Fig. 13) exhibit not only values of Ri of less than 0.25, but also negative values of up to -30. Since the velocity gradient term in the equation used to compute the Ri number is squared, the negative sign must come from the numerator or static stability term. Although density inversions or reversals are not common at greater depths, active interaction of surface water types can produce lenses or parcels of water that possess smaller density than the immediately surrounding water, and thereby produce the negative static stability. Such reversals normally exist but for short periods of time since the parcel will immediately begin to ascend to come into density equilibrium with the surrounding water. The warm frontal interface or trapped lense of water (shown in Fig. 6) shows a density inversion at 05:00 ~ 07:00 and again at 10:00 ~ 11:00. This density inversion will be a site of active mixing and turbulence until the density anomaly is eliminated.

Dynamic instability as evidenced by very small and sometimes negative Ri numbers dominates the observation period of station 4 (Fig. 14). Water of nearly neutral density is common in the upper 10 m according to the sigma-t time series. Although a slight pycnocline does exist (23.8 ~23.9), the velocity shear is sufficient apparently the still keep the Ri number small.

Turbulent dispersion

Because turbulent or eddy diffusion plays an important role in observed distributions of physical and biological parameters, experiments conducted at two different locations estimate the magnitude of turbulent diffusion (Fig. 15). One experiment was conducted in the vicinity of fixed station 2, while the second experiment was made in a protected embayment of Ilha Grande.

The technique used involved an initial dispersal of a known quantity of fluorescent dye solution. After dispersal, temporal and spatial changes in the dye patch were made by taking water samples for a period of time in order to allow the turbulent energy present in the water to disperse the initial path of dye. Rhodamine B dye was selected for use because its fluorescence emmission is more efficient than that of other common dyes such as Fluorescein. Smaller concentrations therefore, could be dispersed and subsequently detected during the field experiments. Another reason for the choice was that Rhodamine B is less affected by adsorption onto suspended sediment than Fluorescein (Stevenson,

1966). Because the fluorometer only measures relative concentration (or fluorescence), it was necessary to calibrate the instrument prior to field work.

A calibration curve for Rhodamine B dye was determined in the laboratory from several known dye concentrations, for a turner fluorometer (Model 111). A sensitivity of 3X, combined with a neutral filter of 10%, a primary filter of 0.546 microns and a secondary filter of 0.570 microns were used to make determinations. Measurements were made at an ambient temperature of 22.2°C.

During each experiment the turner fluorometer aboard a little vessel was used to measure the dye fluorescence. A suction pump ($\frac{1}{4}$ HP capacity) was used to pump sea water to the continuous flow cell of the fluorometer. A continuous strip chart record of fluorescence was thereby obtained during each experiment. In order to determine the location of the Rhodamine B measurements, the small vessel was continually tracked by radar aboard the nearly R/V "Prof. W. Besnard".

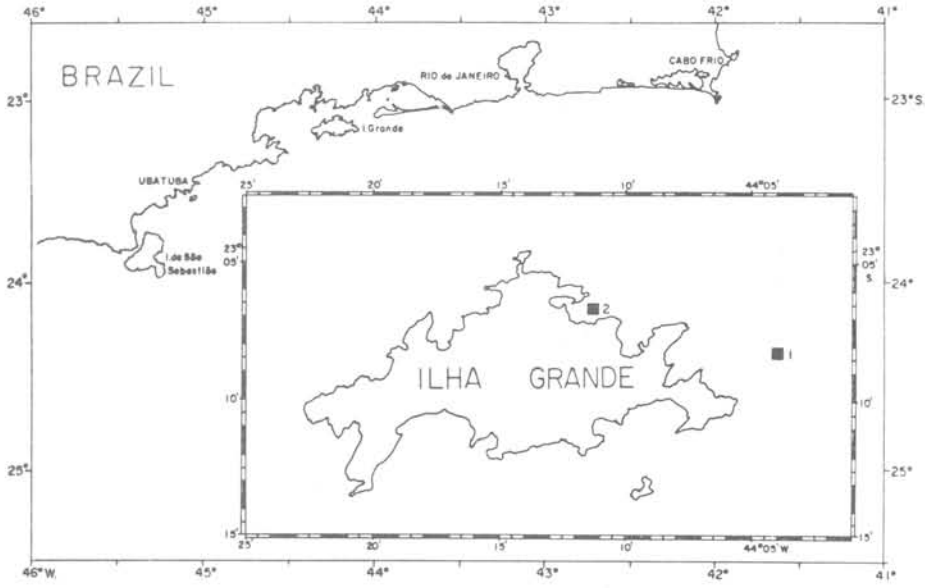

Fig. 15. Dye release points.

From the calibration curve noted above, we determined the dye concentrations, which were then plotted as a function of distance from the dispersal point (Fig. 16). Results from both experiments are shown in this Figure. The first experiment made near station 1/2 began at 09:30 and finished at 10:35. The second experiment beginning at 13:35 and finishing at 14:27, took place in Enseada do Saco do Céu. From the maximum known concentrations for the two experiments, we estimated the horizontal diffusion coefficient K, using Ichiye's model, modified by Stevenson (1966):

$$S = \frac{M}{4\pi K t} \exp \frac{-(x-ut)^2-(y-vt)^2}{4 Kt} \qquad (3)$$

where: M - the initial dye mass,
K - the horizontal diffusion constant is considered equal to the component constants

$$K = K_x = K_y$$

t - elapsed time after dye dispersal
u, v - velocity components
S - the dye concentration at any time after dispersal.

In the first experiment 112,4 g of Rhodamine B were dispersed. The experimental results are shown for the more representative time intervals of the full experiment, during which time 6 transects were made across the dye patch (Fig. 16). The results of these samples provide an estimate of $K = 9 \times 10^3 \text{ cm}^2 \text{ s}^{-1}$.

The second experiment was made in more protected water of Enseada do Saco do Céu and 30 g of dye was dispersed. The experimental results of 5 transects covering a period of 5 minutes are shown for the smaller dye patch (Fig. 16). From the second experiment, K was estimated to be = 3,5 x 10^3 cm^2 s^{-1}. A comparison of the results from the first dye experiment with the static stability and Richardson number data (Fig. 12) shows that the dye experiment was made during a relatively more turbulent regime than either before or after the dye experiment was actually made. Because no hydrographic data were available for the site of the second dye experiment it is not possible to directly compare the dye dispersion results with static and dynamic stability values. It is not unexpected that the value of K for the Enseada do Saco do Céu is smaller than for the station 1/2 site, since the embayment area is more protected from the winds and currents than station 1/2 receives.

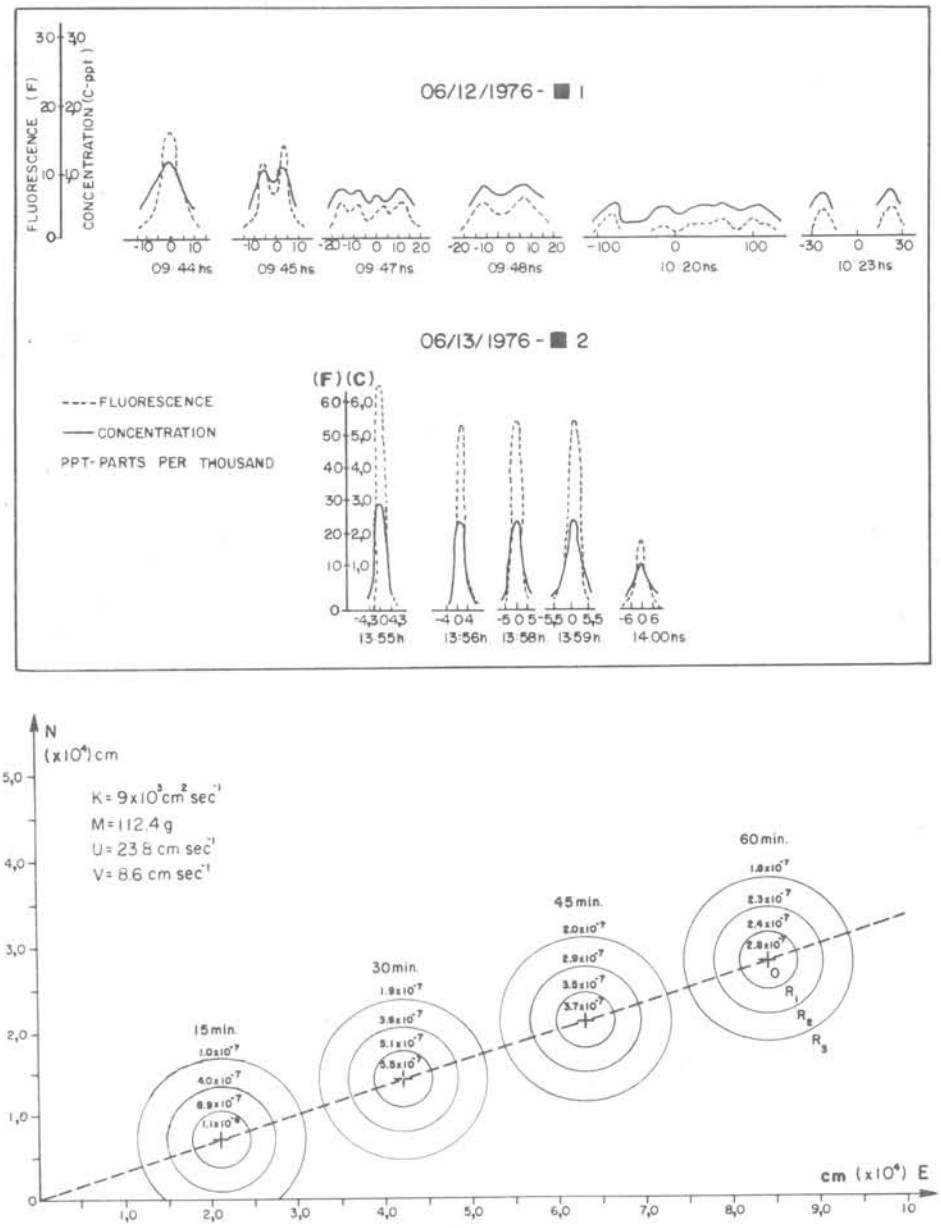

Fig. 16. Dye concentration measured across the dispersal points and dye concentration dispersion taking in consideration diffusive and advective aspects.

Although the transects were not made across the dye patches from different angles, the transects that were completed show the concentration levels to have been reasonably symmetric on either side of the assumed center of the dye patches. This near-symmetry suggests that horizontal current shear was either zero or very small and that $K_x = K_y$. Longer observation periods, however, might have shown that such homogeneities do no persist. Small anisotropicities are present as shown by slight irregularities with increasing distance from the centers of the dye patches.

This simple 2-dimensional diffusion model shows that the peak concentration level at an elapsed time of 15 minutes decreases to only about 34% of this concentration at an elapsed time of 45 minutes (a time difference of 30 minutes). While the concentration levels are not the same between the model and the actual measurements, the reduction in peak concentration from the first transect to one 36 minutes later, resulted in a decrease of about 38%, very similar to that derived from the model calculations.

Using the same input data used to generate the simulated dye patches in Figure 16 (lower panel), calculations were also made with the model to determine the dye concentration as a function of time for set distances from the point of origin (Fig. 17). The center point of the dye patch uses a Lagrangian reference. That is, the concentration curves are referenced to the center of the patch that in turn possesses an advection velocity (V_x = 23.8 cm s^{-1}, V_y = 8.6 cm s^{-1}). Figure 17 suggests among other things that the time rate of change of dye concentration is most rapid initially and the decays assymptotically. Frequently the center position of the patch is difficult to determine, althouh aerial photography can greatly assist in this aspect (Carter & Okubo, 1965). While the aerial photographs of the dye patches are not in or of themselves quantitative data, they aid in the delineation of the perimeter of the patches and in indicating the presence of current shears. From a series of studies of partially or completely protected rivers and lagoons, Carter & Okubo (1965) estimate a horizontal coefficiente K of about 4×10^3 cm^2 s^{-1} during the early part of their experiments, using a slightly different diffusion equation. Although the two dye experiments discussed in this paper were brief in duration, the information gained from them suggests that more dye dispersal experiments of greater duration can be planned for the future in the coastal zone of Brazil.

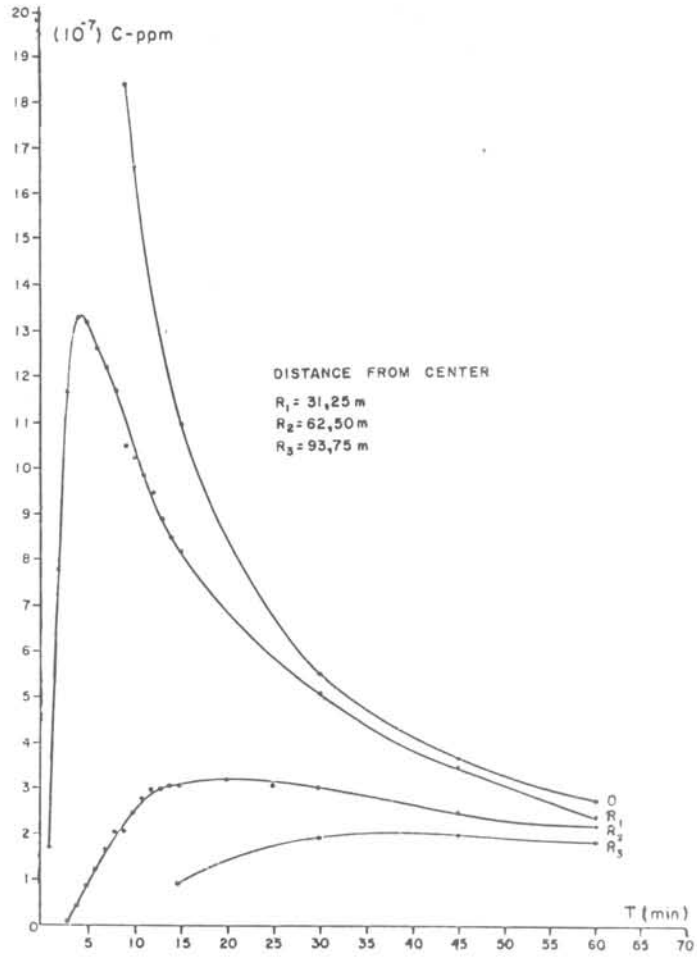

Fig. 17. Dye concentration variation with increase time and distance from dispersal points. Concetration lines correspond to distances rings in Fig. 16 and use unitial dye quantity of first experiment.

Conclusions

Based on the seasonal data of the February and June/1976 cruises we are able to make the following concluding remarks:

1 - Differences in temperature, salinity and sigma-t exist between the two seasons, with the summer season having higher temperatures (4.0°C), smaller salinity (0.9°/oo) and smaller sigma-t (1.8);

2 - Current meter measurements at 4 fixed stations show the currents to undergo strong fluctuations. Short period oscillations or pulses (ca. 1-1.1 hour period) as well as tidal flows are present. Observations show significant differences between the stations due principally to location of the stations;

3 - As comparison of hydrographic and current meter data suggest the frequent passage of fronts separating oceanic water from coastal water. Rapid reversals in the current were usually associated with the frontal interfaces passage;

4 - Examination of static stability (Brunt-Väisälä frequency) shows that the water column in February was much more stable than in June for the same location. Density inversions (reversals in density with increasing depth) often occurred at the stations in June, indicating a pronounced tendency for overturn of the water column;

5 - Richardson numbers during February, on the other hand, showed a tendency for instability due to velocity shears in the present with the passage of frontal feature. The combination of density inversions, coupled with vertical velocity shears during June showed much of the water column to be highly unstable at that time;

6 - The magnitude of horizontal diffusion was estimated from two dye dispersal experiments. The first experiment was made to the east of Ilha Grande and provided a diffusion coefficient K of 9×10^3 cm^2 s^{-1}. A second experiment conducted in more protected water of Enseada do Saco do Céu yielded an estimate of 3.5×10^3 cm^2 s^{-1}. The estimate of 9×10^3 cm^2 s^{-1} was obtained during a relatively more turbulent observational period corresponding to the small (or negative) Brunt-Väisälä and Richardson number values.

Acknowledgments

The basic data and preparation of this paper was supported by the OAS Program: Programa Multinacional de Ciências do Mar, Project "Integrado para o Uso e Exploração Racional do Meio Ambiente Marinho/Subprojeto Biologia da Pesca" - FINEP and São Paulo University. Ours thanks to Mr. Marco Antonio Montalban and Mr. Osmar M. P. Campos for the drawings and to Miss Marilza Correia and Ms. Eliete A. O. Maciel for typing the manuscript. Support for Merrit Stevenson was provided by the Instituto de Pesquisas Espaciais/CNPq, São José dos Campos, SP, and it is acknowledged with appreciation.

References

BRASIL. DIRETORIA DE HIDROGRAFIA E NAVEGAÇÃO. 1974. Oceano Atlântico: carta piloto de Trinidad ao Rio da Prata. Observações efetuadas pela Marinha do Brasil de 1951 a 1972. Projeção Mercator. Escala natural 1:10.000.000 na lat. 12°30'S. Atlas Cartas Piloto (14.200).

1975. Tábuas das marés para o ano de 1976. DG 16-13, 197p.

CARTER, H. H. & OKUBO, A. 1965. A study of the physical processes of movement and dispersion in the Cape Kennedy area. Chesapeake Bay Institute, The Johns Hopkins University. Rep. nº NYC-2973-1; Ref. 65-2. 150p. + appendix.

IKEDA, Y. & STEVENSON, M. R. 1978. Time series analysis of NOAA-4 sea surface temperature (SST) data. Remote Sensing Environm., 7(4):349-360.

---------- 1980. Determination of circulation and short period fluctuation at Ilha Grande Bay (RJ) - Brazil. Bolm Inst. oceanogr., S Paulo, 29(1):89-98.

MIRANDA, L. B. de & IKEDA, Y. 1976. Investigación preliminar de la variabilidad de temperatura y salinidad superficiales en la region adyacent a Bahia de Isla Grande (RJ) 16/06 a 21/06/1975. *In*: Pérez-Rodríguez, R. & Suárez-Zozaya, M. R., ed. - Reunión Latinoamericana sobre Ciencia y Tecnologia de los oceanos, I, del 26 de mayo al 1º de junio de 1976. México, D.F., Secretaria de Marina, p. 15-48.

MIRANDA, L. B. de & IKEDA, Y.; CASTRO FILHO, B. M. de & PEREIRA FILHO, N. 1977. Note of the occurrence of saline fronts in the Ilha Grande (RJ) region. Bolm Inst. oceanogr., S Paulo, 26(2):249-256.

PHILLIPS, O. M. 1966. The dynamics of the upper ocean. Cambridge, University Press, 261p.

SIGNORINI, S. R. 1980*a*. A study of the circulation in Bay of Ilha Grande and Bay of Sepetiba. Part 1. A survey of the circulation based on experimental field data. Bolm Inst. oceanogr., S Paulo, 29(1):41-55.

SIGNORINI, S. R. 1980*b*. A study of the circulation in Bay of Ilha Grande and Bay of Sepetiba. Part II. An assessment to the tidally and wind-driven circulation using a finite element numerical model. Bolm Inst. Oceanogr., S Paulo, 29(1):57-68.

SMITH, R. L. 1978. Poleward propagating perturbations in currents and sea levels along the Peru coast. J. geophys. Res., 83(C12):6083-6092.

STEVENSON, M. 1966. Subsurface currents of the Oregon coast. Ph. D. Thesis. Oregon State University, 140p.

TOMMASI, L. R.; VALENTE, M. T. M. & ACEDO, R. 1972. Cephalochordata da região da Ilha Grande (RJ). Bolm Inst. oceanogr., S Paulo, 21:149-162.

(Manuscript received on 15/Oct./1979; accepted on 25/Nov./1981)